Supporting Information for

Gold nanoparticle-PPE constructs as biomolecular material mimics: Understanding the electrostatic and hydrophobic interactions

Ronnie L. Phillips,[†] Oscar R. Miranda,[‡] David E. Mortenson,[‡] Chandramouleeswaran Subramani, [‡] Vincent M. Rotello,[*,‡] Uwe H.F. Bunz[*,†]

[†] *School of Chemistry and Biochemistry, Georgia Institute of Technology, 901 Atlantic Drive, Atlanta, Georgia 30332*
[‡]*Department of chemistry, University of Massachusetts, 710 North Pleasant Street, Amherst, Massachusetts 01003*

E-mail: uwe.bunz@chemistry.gatech.edu; rotello@chem.umass.edu

Materials and Methods: Swallowtail-substituted carboxylate PPE (**Sw-CO_2**) was synthesized according to published procedure.[1] Fluorescence intensity changes at 465 nm were recorded in 96-well plates (300 μL Whatman® Glass Bottom microplate) on a Molecular Devices SpectraMax M5 micro plate reader with an excitation wavelength of 405 nm. Phosphate buffer (PB), phosphate buffered saline (PBS), piperazine-1,4-bis(2-ethanesulfonic acid) (PIPES), N-2-hydroxyethylpiperazine-N'-2-ethanesulfonic acid (HEPES), and tris(hydroxymethyl)aminomethane hydrochloride (Tris-HCl) were purchased from Sigma-Aldrich. The buffers were diluted to a concentration of 5 mM and a pH of 7.2 with DI H_2O. To calculate log P, computational program Maestro 8.0 was used.

Scheme S1. Synthesis of Ligands[2]

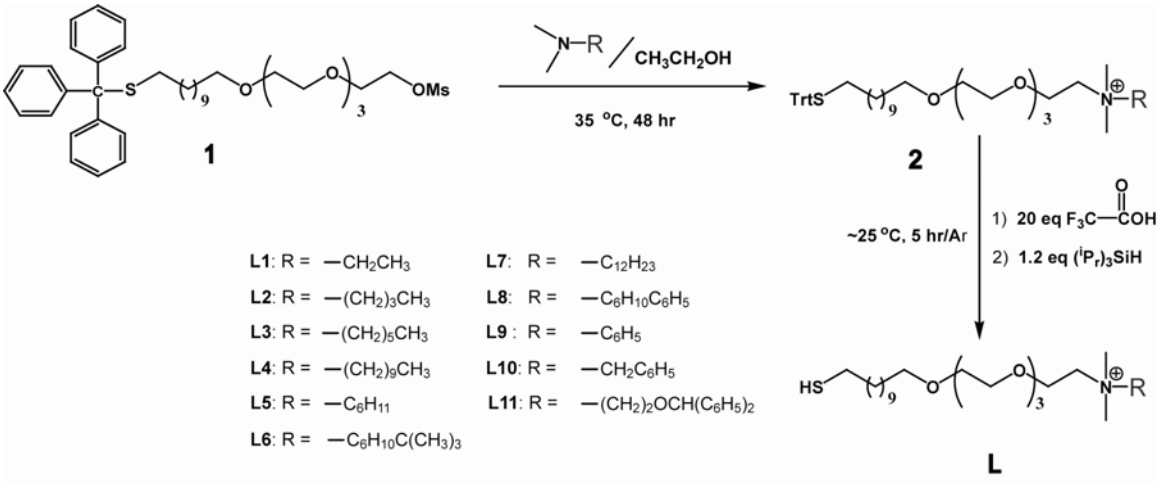

General procedure: Compound **2** bearing ammonium end groups were synthesized through the reaction of 1,1,1-triphenyl-14,17,20,23-tetraoxa-2- thiapentacosan-25-yl methanesulphonate (**1**) with corresponding substituted N,N-dimethylamines during 48 h at ~35 ^{o}C. The trityl protected thiol ligand **(2)** was dissolved in dry dichloromethane (Methylene Chloride, DCM) and an excess of trifluoroacetic acid (TFA, ~ 20 equivalents) was added. The color of the solution was turned to yellow immediately. Subsequently, triisopropylsilane (TIPS, ~ 1.2 equivalents) was added to the reaction mixture. The reaction mixture was stirred for ~5 h under Ar condition at room temperature. The solvent and most TFA and TIPS were distilled off under reduced pressure. The pale yellow residue was further dried in high vacuum. The product (**L**) formation was quantitative and their structure was confirmed by NMR. The yields were >95%.

Compound **L1**: ^{1}H NMR (400MHz, $CDCl_3$, TMS): δ 3.94 (br, 2H, -OC$\underline{H_2}$-(CH_2N)-), 3.69-3.56 (m, 14H, -CH_2O- + -CH_2N-), 3.44 (t, 2H, -CH_2O-), 3.40-3.32 (m, 2H,-NCH_2-), 3.23 (s, 6H, -(CH_3)$_2$N-), 2.78 (s, 3H, -$CH_3SO^-_3$-), 2.51 (q, 2H, -CH_2S-), 1.69-1.149 (m, 4H, (SCH_2)C$\underline{H_2}$ + -C$\underline{H_2}$(CH_2O)-) , 1.44-1.24 (m, 18H, -SH + -CH_2- + -(NCH_2)C$\underline{H_3}$).

Compound **L2**: ^{1}H NMR (400MHz, $CDCl_3$, TMS): δ 3.96 (br, 2H, -OC$\underline{H_2}$-(CH_2N)-), 3.68-3.57 (m, 14H, -CH_2O- + -CH_2N-), 3.49 (t, 2H, -CH_2O-), 3.39-3.33 (m, 2H,-NCH_2-), 3.17 (s, 6H, -(CH_3)$_2$N-), 2.91 (s, 3H, -$CH_3SO^-_3$-), 2.52 (q, 2H, -CH_2S-), 1.78-1.52 (m, 6H, -(NCH_2)C$\underline{H_2}$-) + (SCH_2)C$\underline{H_2}$ + -C$\underline{H_2}$(CH_2O)-) , 1.44-1.24 (m, 17H, -SH + -(NCH_2CH_2-)C$\underline{H_2}$-) + -CH_2-), 0.98 (t, 3H, - CH_3-).

Compound **L3**: ^{1}H NMR (400MHz, $CDCl_3$, TMS): δ 3.95 (br, 2H, -OC$\underline{H_2}$-(CH_2N)-), 3.68-3.56 (m, 14H, -CH_2O- + -CH_2N-), 3.46 (t, 2H, -CH_2O-), 3.40-3.33 (m, 2H,-NCH_2-), 3.19 (s, 6H, -(CH_3)$_2$N-), 2.87 (s, 3H, -$CH_3SO^-_3$-), 2.52 (q, 2H, -CH_2S-), 1.76-1.53 (m, 6H, -(NCH_2)C$\underline{H_2}$-) + (SCH_2)C$\underline{H_2}$ + -C$\underline{H_2}$(CH_2O)-) , 1.41-1.22 (m, 21H, -SH + -(NCH_2CH_2-)C$\underline{H_2}$-) + -CH_2-), 0.89 (t, 3H, - CH_3-).

Compound **L4**: ^{1}H NMR (400MHz, $CDCl_3$, TMS): δ 3.94 (br, 2H, -OC$\underline{H_2}$-(CH_2N)-), 3.67-3.54 (m, 14H, -CH_2O- + -CH_2N-), 3.48 (t, 2H, -CH_2O-), 3.41-3.32 (m, 2H,-NCH_2-), 3.17 (s, 6H, -(CH_3)$_2$N-), 2.90 (s, 3H, -$CH_3SO^-_3$-), 2.51 (q, 2H, -CH_2S-), 1.78-1.52 (m, 6H, -(NCH_2)C$\underline{H_2}$-) + (SCH_2)C$\underline{H_2}$ + -C$\underline{H_2}$(CH_2O)-) , 1.45-1.15 (m, 29H, -SH + -(NCH_2CH_2-)C$\underline{H_2}$-) + -CH_2-), 0.87 (t, 3H, - CH_3-).

Compound **L5**: ^{1}H NMR (400MHz, $CDCl_3$, TMS): δ3.95 (br, 2H, -OC$\underline{H_2}$-(CH_2N)-), 3.81-3.72 (m, 1H, H_{Cyclo}), 3.69-3.53 (m, 14H, -CH_2O- + -CH_2N-), 3.49 (t, 2H, -CH_2O-), 3.11 (s, 6H, -(CH_3)$_2$N-),

2.91 (s, 3H, -$CH_3SO^-_3$-), 2.52 (q, 2H, -CH_2S-), 2.23 (d, 2H, H_{Cyclo}), 1.99 (d, 2H, H_{Cyclo}), 1.78-1.52 (m, 4H, -(SCH_2)C$\underline{H}_2$ + -C$\underline{H}_2$(CH_2O)-), 1.51-1.12 (m, 21H, SH + -CH2- + H_{Cyclo}).
Compound **L6**: ^{1}H NMR (400MHz, $CDCl_3$, TMS): δ 3.96 (br, 2H, -OC$\underline{H}_2$-(CH_2N)-), 3.79-3.75 (m, 1H, H_{Cyclo}), 3.66-3.57 (m, 14H, -CH_2O- + -CH_2N-), 3.46 (t, 2H, -CH_2O-), 3.12 (s, 6H, -$(CH_3)_2N$-), 2.89 (s, 3H, -$CH_3SO^-_3$-), 2.52 (q, 2H, -CH_2S-), 2.28 (d, 2H, H_{Cyclo}), 2.01 (d, 2H, H_{Cyclo}), 1.64-1.54 (m, 4H, -(SCH_2)C$\underline{H}_2$ + -C$\underline{H}_2$(CH_2O)-), 1.47 (q, 2H, H_{Cyclo}), 1.33 (t, ^3J = 8.0 Hz, 1H, -SH), 1.30-1.22 (m, 14H, -CH2-), 1.16 (q, 2H, H_{Cyclo}) 1.04 (td, 1H -CHC-), 0.86 (s, 9H, -$C(CH_3)_3$-).

Compound **L7**: ^{1}H NMR (400MHz, $CDCl_3$, TMS): δ 3.98 (br, 2H, -OC$\underline{H}_2$-(CH_2N)-), 3.78-3.75 (m, 1H, H_{Cyclo}), 3.64-3.55 (m, 14H, -CH_2O- + -CH_2N-), 3.46-3.42 (dt, 2H, -CH_2O-), 3.16 (s, 6H, -$(CH_3)_2N$-), 2.86 (s, 3H, -$CH_3SO^-_3$-), 2.52 (q, 2H, -CH_2S-), 1.93-1.40 (m, 26H, SCH_2)C$\underline{H}_2$ + -C$\underline{H}_2$(CH_2O)- + H_{Cyclo}), 1.33 (t, ^3J = 7.82 Hz, 1H, -SH), 1.29-1.24 (m, 14H, -CH2-).

Compound **L8**: ^{1}H NMR (400MHz, $CDCl_3$, TMS): δ 7.4-7.2 (m, 4H, H_{Ar}), 7.17 (d, 1H, H_{Ar}), 3.95 (d and br, 2H, -OC$\underline{H}_2$-(CH_2N)-), 3.79-3.52 (m, 14H, -CH_2O- + -CH_2N-), 3.45 (q, 2H, -CH_2O-),3.29-3.22 (m and br, 1H, H_{Cyclo}), 3.01-2.92 (m and br, 1H, H_{Cyclo}) 2.87 (s, 3H, -$CH_3SO^-_3$-), 2.81 (d and br, 6H, -$(CH_3)_2N$-), 2.52 (q, 2H, -CH_2S-), 2.39-2.26 (m, 2H, H_{Cyclo}), 2.19-2.06 (m, 2H, H_{Cyclo}), 1.96-1.84 (m, 4H, H_{Cyclo}), 1.72-1.53 (m, 4H, -(SCH_2)C$\underline{H}_2$ + -C$\underline{H}_2$(CH_2O)-), 1.42-1.1.19 (m, 15H, -SH + -CH_2-).

Compound **L9**: ^{1}H NMR (400MHz, $CDCl_3$, TMS): δ 7.82 (d, 2H, H_{Ar}), 7.66-7.51 (m, 3H, H_{Ar}), 4.24 (br, 2H, -OC$\underline{H}_2$-(CH_2N)-), 3.78 (s, 6H, -$(CH_3)_2N$-), 3.68-3.52 (m, 14H, -CH_2O- + -CH_2N-), 3.47-3.36 (m, 2H, -CH_2O-), 2.87 (s, 3H, -$CH_3SO^-_3$-), 2.52 (q, 2H, -CH_2S-), 1.70-1.46 (m, 4H, -(SCH_2)C$\underline{H}_2$ + -C$\underline{H}_2$(CH_2O)-), 1.42-1.1.16 (m, 15H, -SH + -CH_2-).

Compound **L10**: ^{1}H NMR (400MHz, $CDCl_3$, TMS): δ 8.37 (d, 1H, H_{Ar}), 7.98 (d, 1H, H_{Ar}), 7.69-7.61 (m, 3H, H_{Ar}), 7.59-7.48 (m, 1H, H_{Ar}), 4.38 (br, 2H,-NCH_2-Ar)), 3.76 (br, 2H, -OC$\underline{H}_2$-(CH_2N)-) 3.72-3.62 (m, 14H, -CH_2O- + -CH_2N-), 3.61-3.55 (m, 2H, -CH_2O-), 3.23 (s, 6H, -$(CH_3)_2N$-), 3.07 (s, 3H, -$CH_3SO^-_3$-), 2.52 (q, 2H, -CH_2S-), 1.67-1.51 (m, 4H, -(SCH_2)C$\underline{H}_2$ + -C$\underline{H}_2$(CH_2O)-), 1.35-1.21 (m, 15H, -SH + -CH_2-).

Compound **L11**: ^{1}H NMR (400MHz, $CDCl_3$, TMS): δ 7.42 (d, 2H, H_{Ar}), 7.37-2.27 (m, 8H, H_{Ar}), 7.25-7.18 (t, 2H, H_{Ar}), 5.13 (s, 1H, H_{Ar}), 4.12 (br, 2H, -CH_2OCAr-), 3.96 (br, 2H, -OC$\underline{H}_2$-(CH_2N)-), 3.64-3.51 (m, 14H, -CH_2O- + -CH_2N-), 3.45 (t, 2H, -CH_2O-), 3.29-3.34 (m, 2H, -NC$\underline{H}_2$(CH_2OCAr), 3.28 (s, 6H, -$(CH_3)_2N$-), 2.86 (s, 3H, -$CH_3SO^-_3$-), 2.52 (q, 2H, -CH_2S-), 1.60-1.48 (m, 4H, -(SCH_2)C$\underline{H}_2$ + -C$\underline{H}_2$(CH_2O)-), 1.34-1.16 (m, 15H, -SH + -CH_2-).

Scheme S2. Synthesis of cationic gold nanoparticles **(NP_1-NP_{11})**

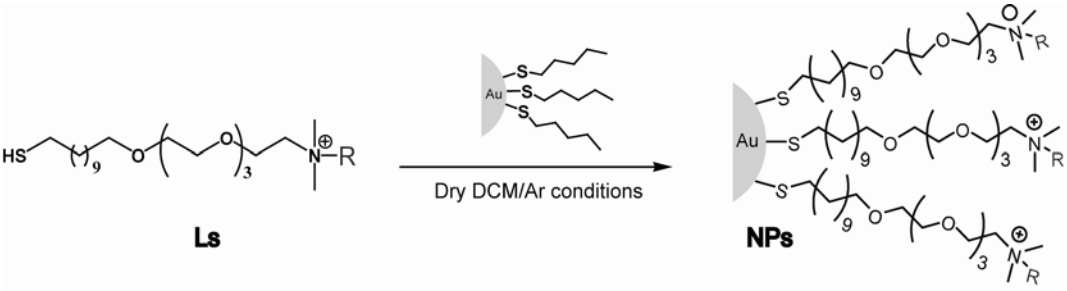

1-Pentanethiol coated gold nanoparticles (*d* = ~2 nm) were prepared according to the previously reported protocol.[3] Place-exchange reaction[4] of compound **Ls** dissolved in DCM with pentanethiol-coated gold nanoparticles (d~2 nm) was carried out for 3 days at environmental temperature. Then, DCM was evaporated under reduced pressure. The residue was dissolved in a small amount of distilled water and dialyzed (membrane MWCO = 1,000) to remove excess ligands, acetic acid and the other salts present with the nanoparticles. After dialysis, the particles were lyophilized to afford a brownish solid. The particles (**NPs**) are redispersed in water and/or ionized water (18 MΩ-cm). ^{1}H NMR spectra in D_2O showed substantial broadening of the proton signals and no free ligands were observed.

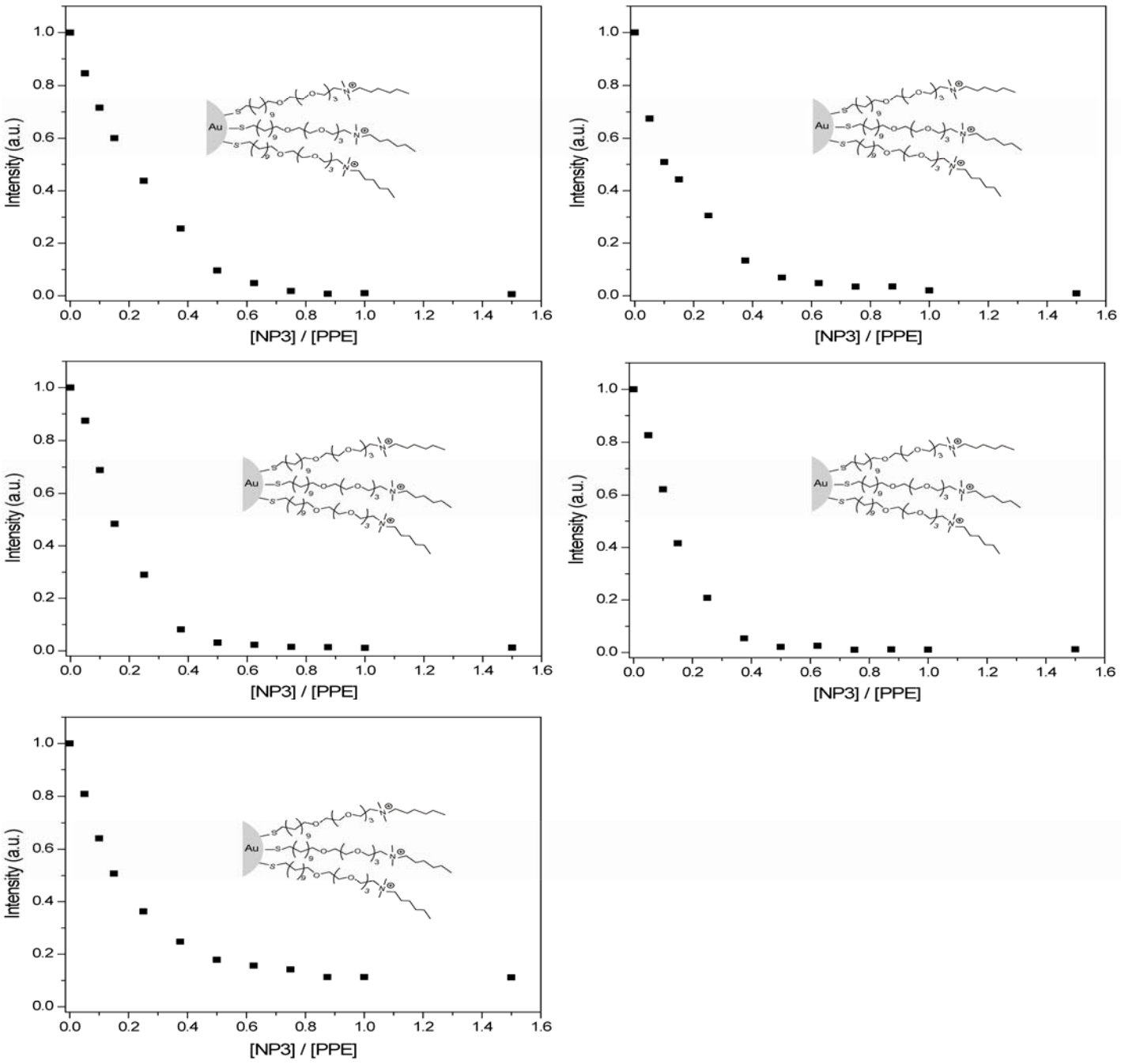

Figure S1. Fluorescence titration curves for the complexation of **NP_3** with **Sw-CO_2** in PB (top left), PIPES (top right), HEPES (middle left), Tris-HCl (middle right), and PBS (bottom left). The changes in fluorescence intensity at 465 nm were measured following the addition of cationic nanoparticles with an excitation wavelength of 405 nm. The complexation of **NP_3** with **Sw-CO_2** in all buffers was similar except in PBS, which disrupted the complexation due to the salt concentration.

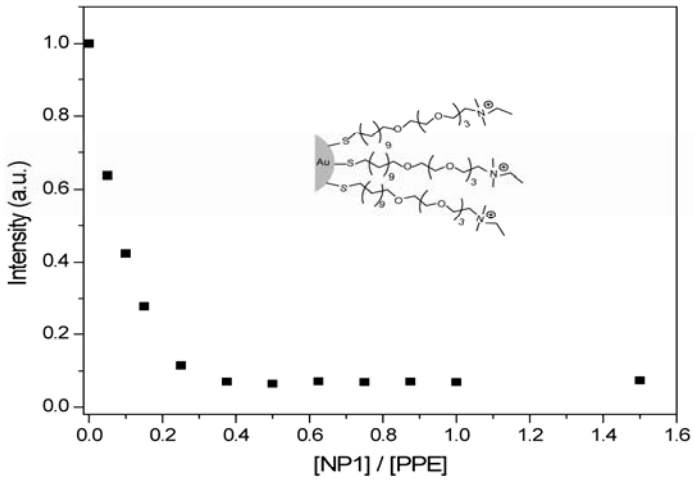
Intensity (a.u.)
[NP1] / [PPE]

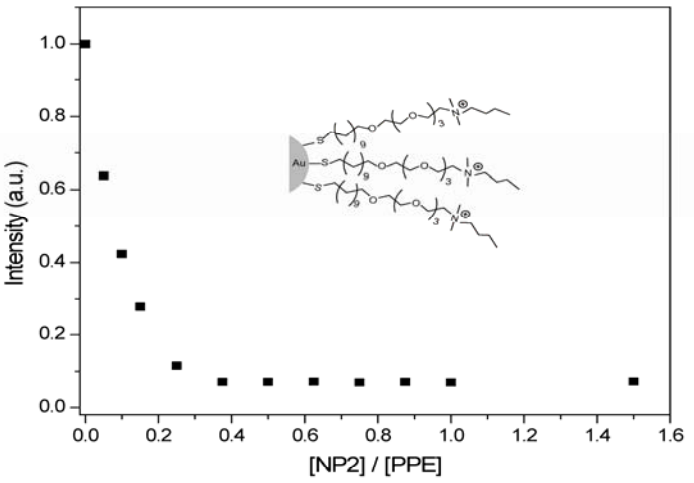
Intensity (a.u.)
[NP2] / [PPE]

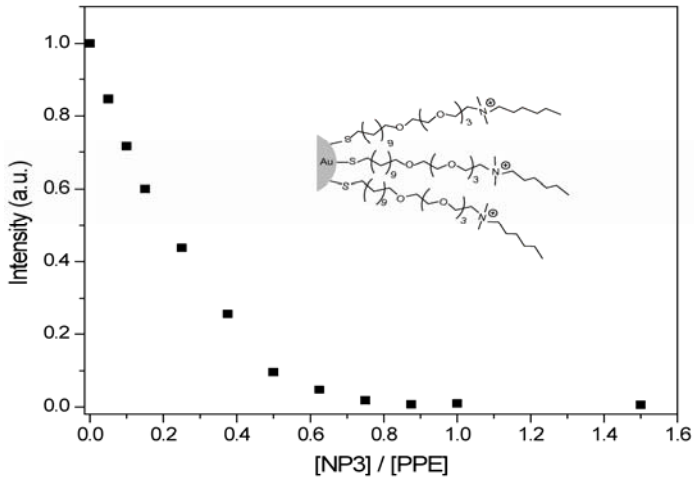
Intensity (a.u.)
[NP3] / [PPE]

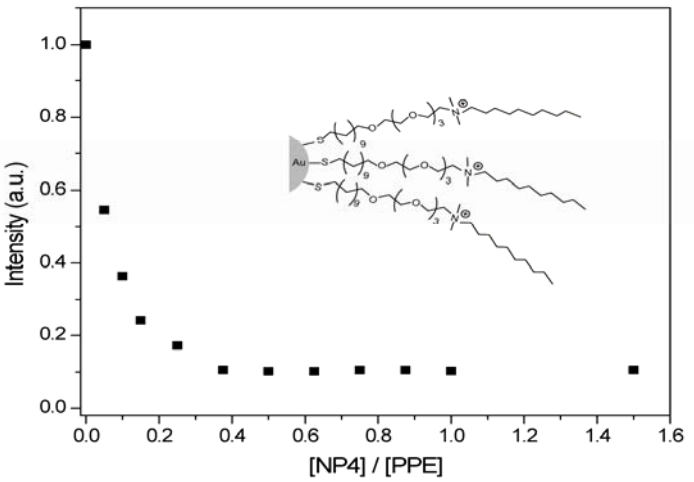
Intensity (a.u.)
[NP4] / [PPE]

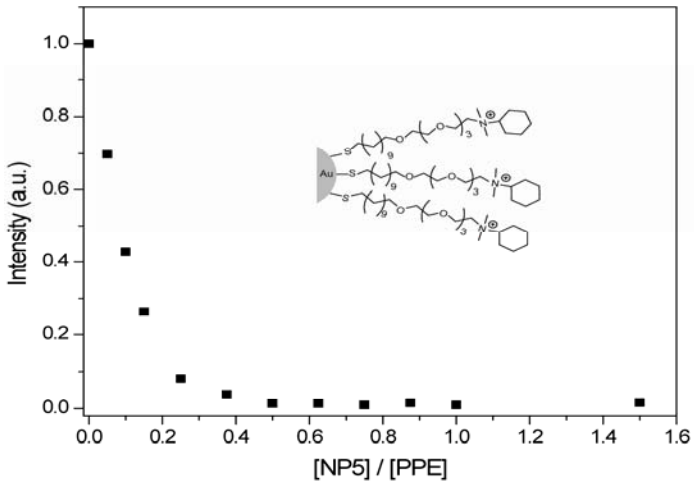
Intensity (a.u.)
[NP5] / [PPE]

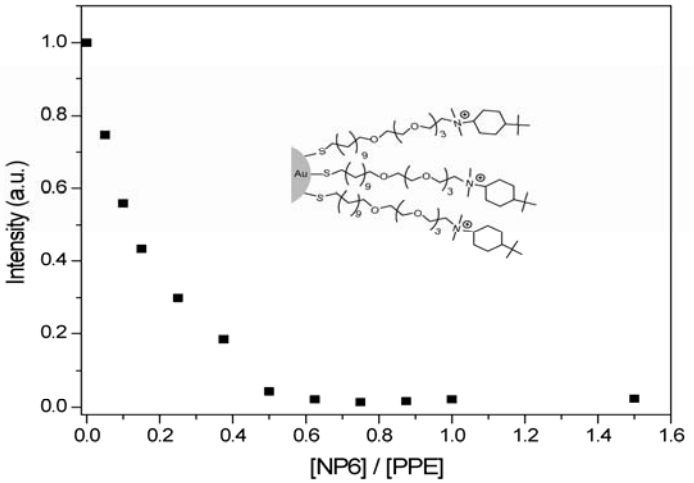
Intensity (a.u.)
[NP6] / [PPE]

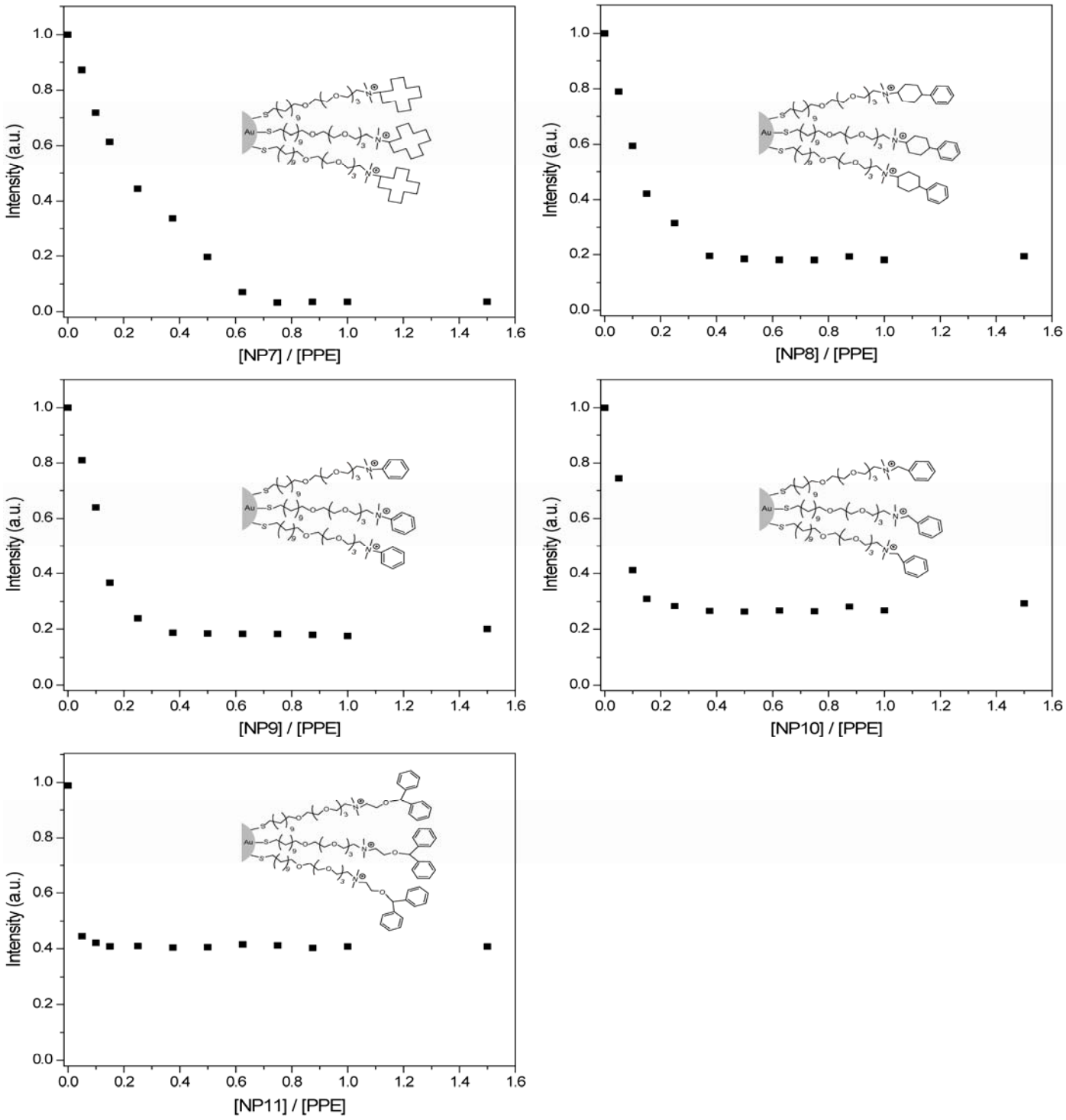

Figure S2. Fluorescence titration curves for the complexation of $\mathbf{NP_1}$-$\mathbf{NP_{11}}$ with $\mathbf{Sw\text{-}CO_2}$ in PB with no NaCl. The changes in fluorescence intensity at 465 nm were measured following the addition of cationic nanoparticles with an excitation wavelength of 405 nm.

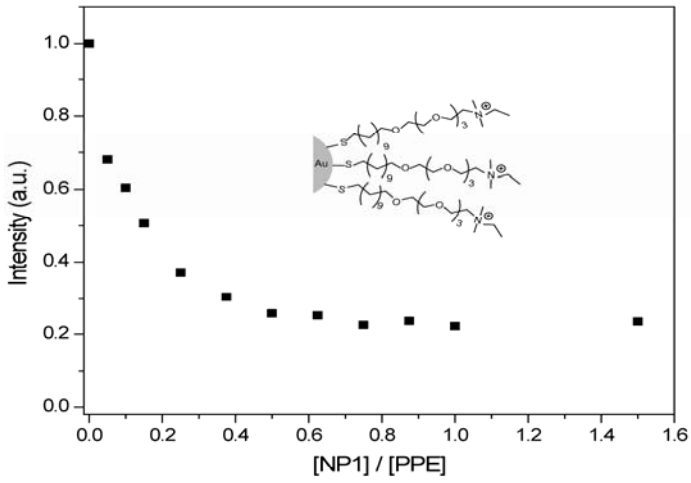
Intensity (a.u.)
[NP1] / [PPE]

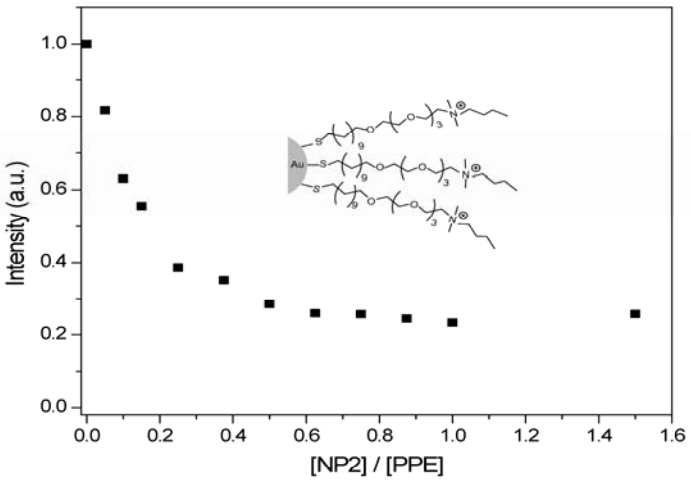
Intensity (a.u.)
[NP2] / [PPE]

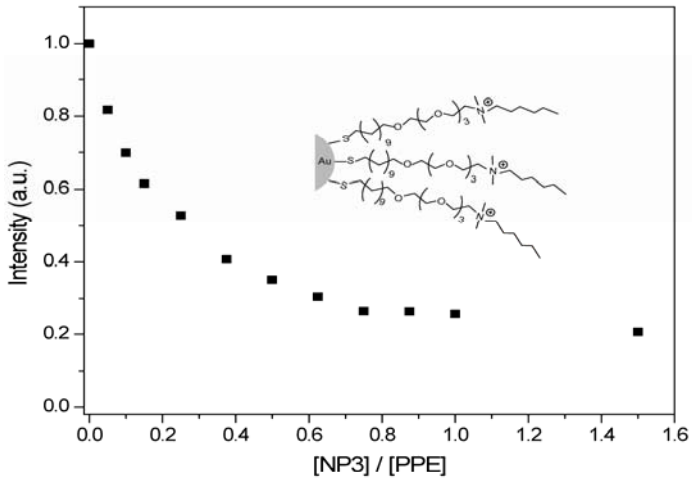
Intensity (a.u.)
[NP3] / [PPE]

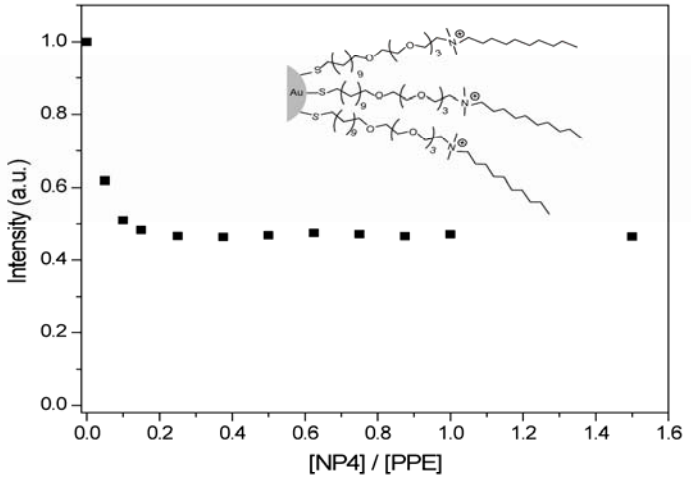
Intensity (a.u.)
[NP4] / [PPE]

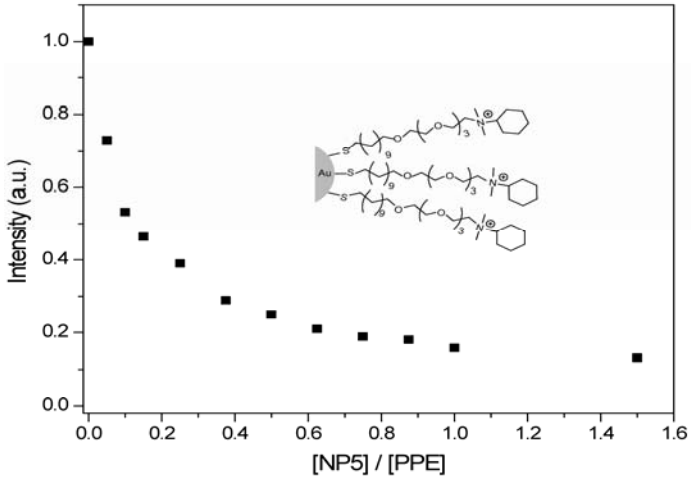
Intensity (a.u.)
[NP5] / [PPE]

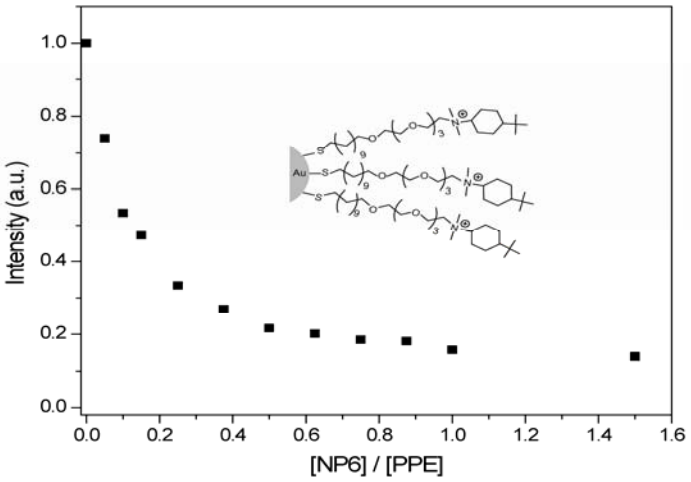
Intensity (a.u.)
[NP6] / [PPE]

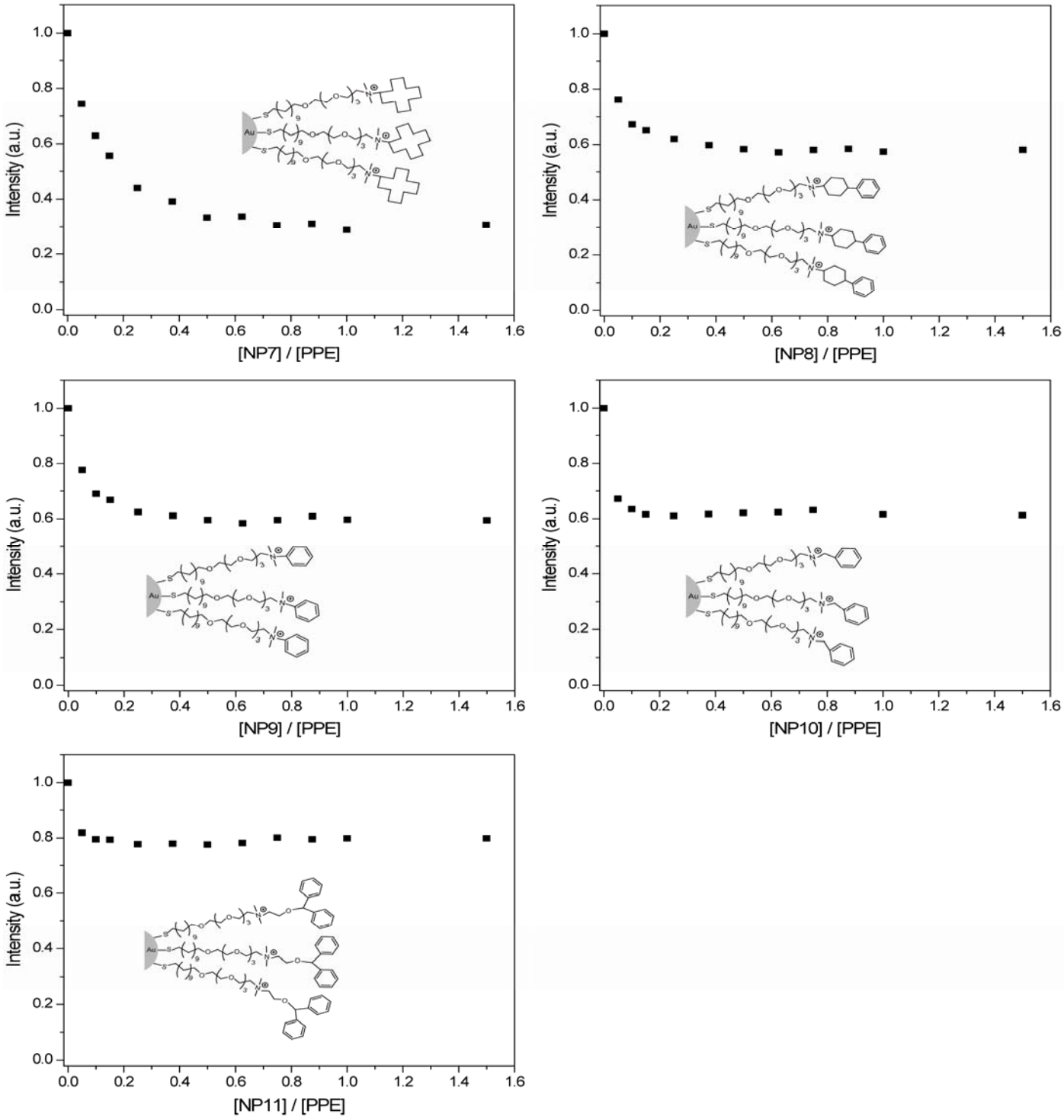

Figure S3. Fluorescence titration curves for the complexation of $\mathbf{NP_1}$-$\mathbf{NP_{11}}$ with $\mathbf{Sw\text{-}CO_2}$ in PB with 100 mM NaCl. The changes in fluorescence intensity at 465 nm were measured following the addition of cationic nanoparticles with an excitation wavelength of 405 nm.

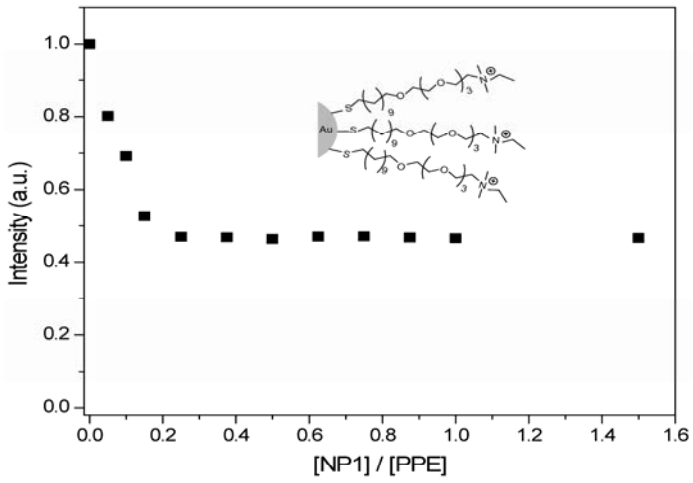
Intensity (a.u.)
[NP1] / [PPE]

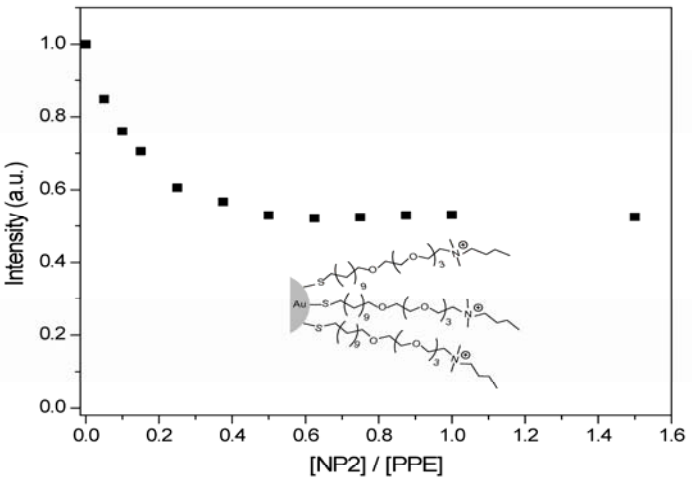
Intensity (a.u.)
[NP2] / [PPE]

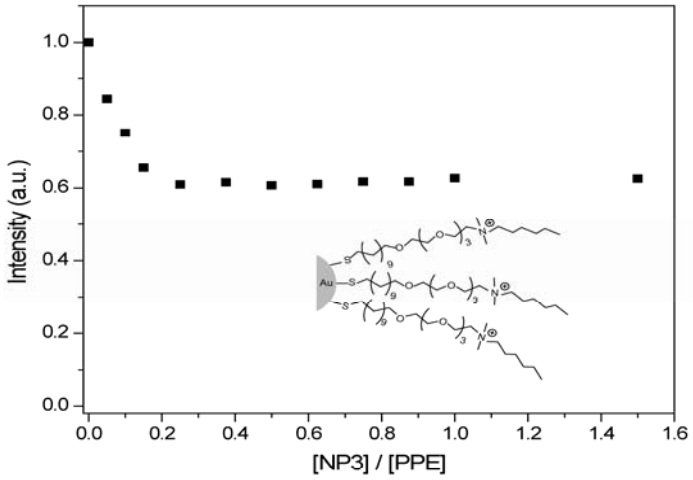
Intensity (a.u.)
[NP3] / [PPE]

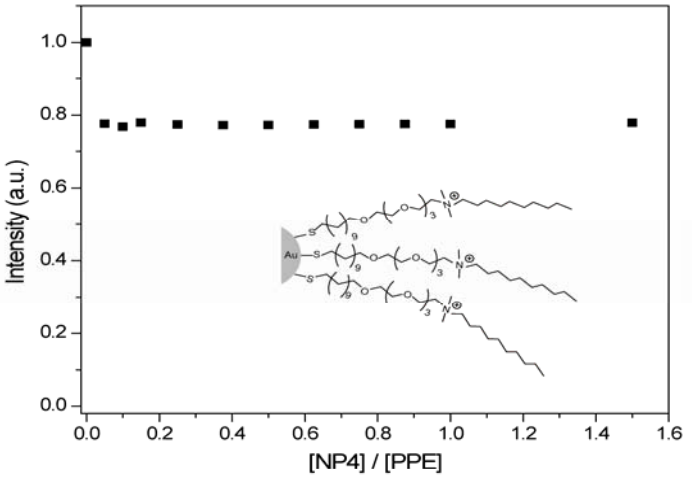
Intensity (a.u.)
[NP4] / [PPE]

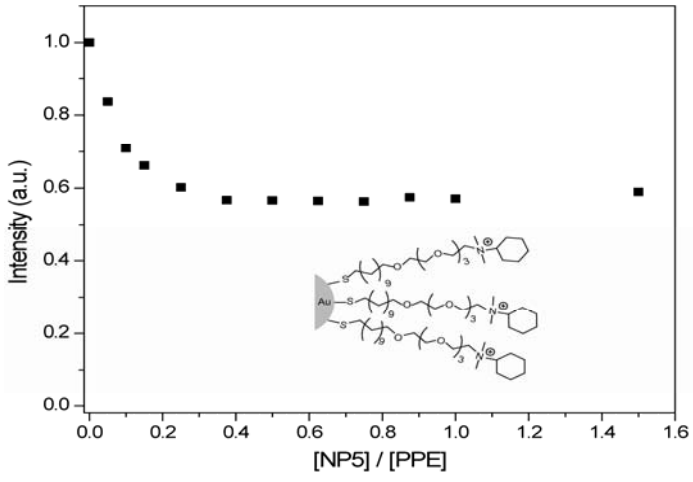
Intensity (a.u.)
[NP5] / [PPE]

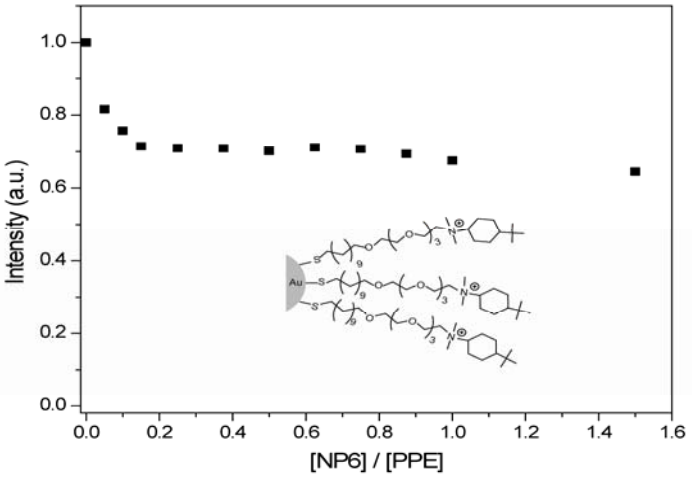
Intensity (a.u.)
[NP6] / [PPE]

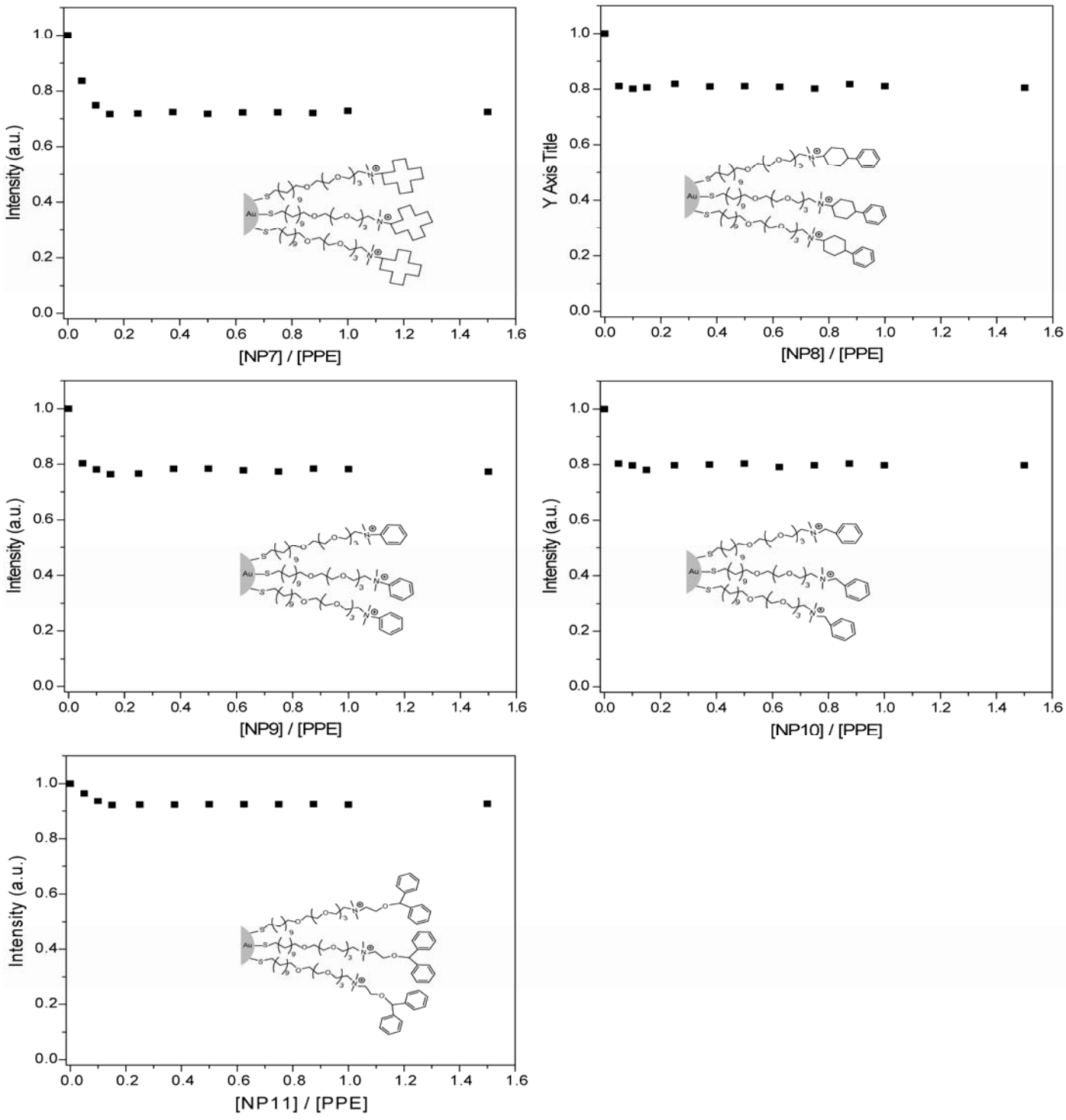

Figure S4. Fluorescence titration curves for the complexation of $\mathbf{NP_1}$-$\mathbf{NP_{11}}$ with $\mathbf{Sw\text{-}CO_2}$ in PB with 250 mM NaCl. The changes in fluorescence intensity at 465 nm were measured following the addition of cationic nanoparticles with an excitation wavelength of 405 nm.

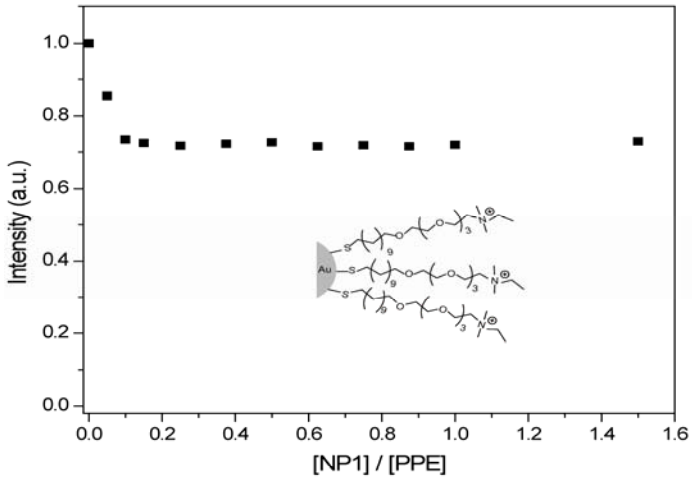
Intensity (a.u.)
[NP1] / [PPE]

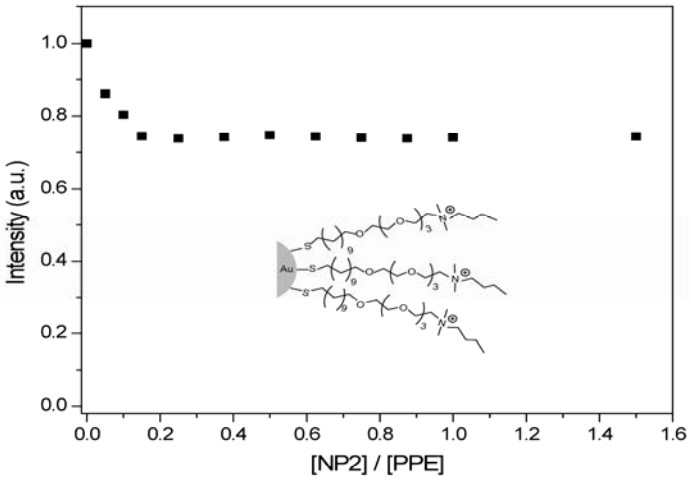
Intensity (a.u.)
[NP2] / [PPE]

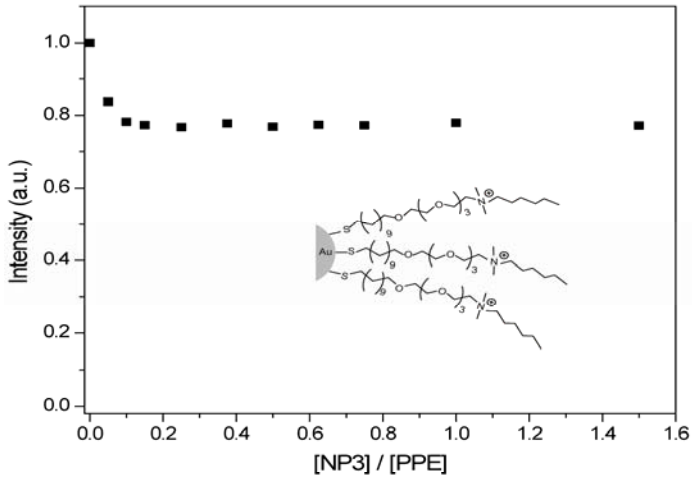
Intensity (a.u.)
[NP3] / [PPE]

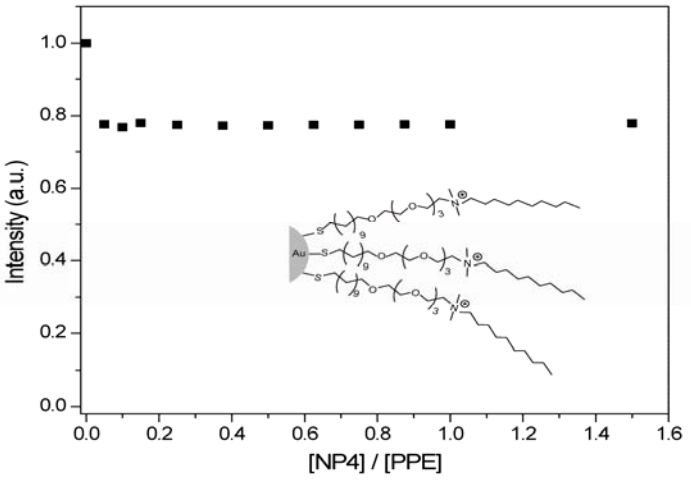
Intensity (a.u.)
[NP4] / [PPE]

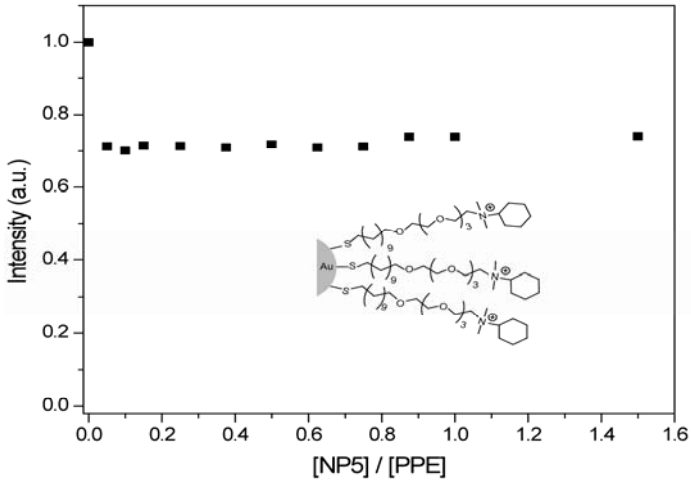
Intensity (a.u.)
[NP5] / [PPE]

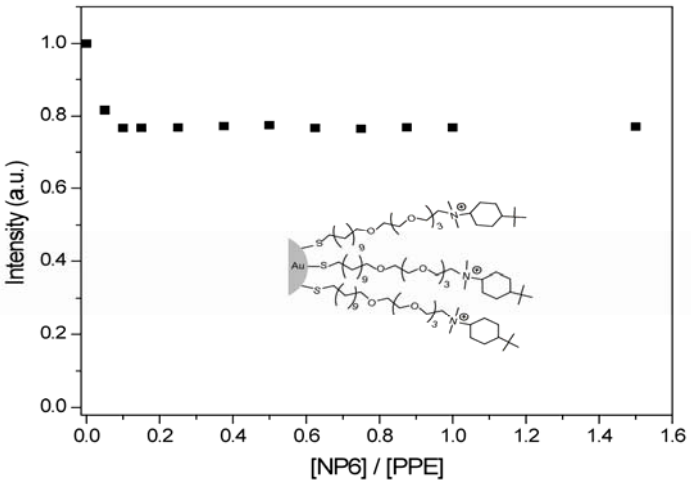
Intensity (a.u.)
[NP6] / [PPE]

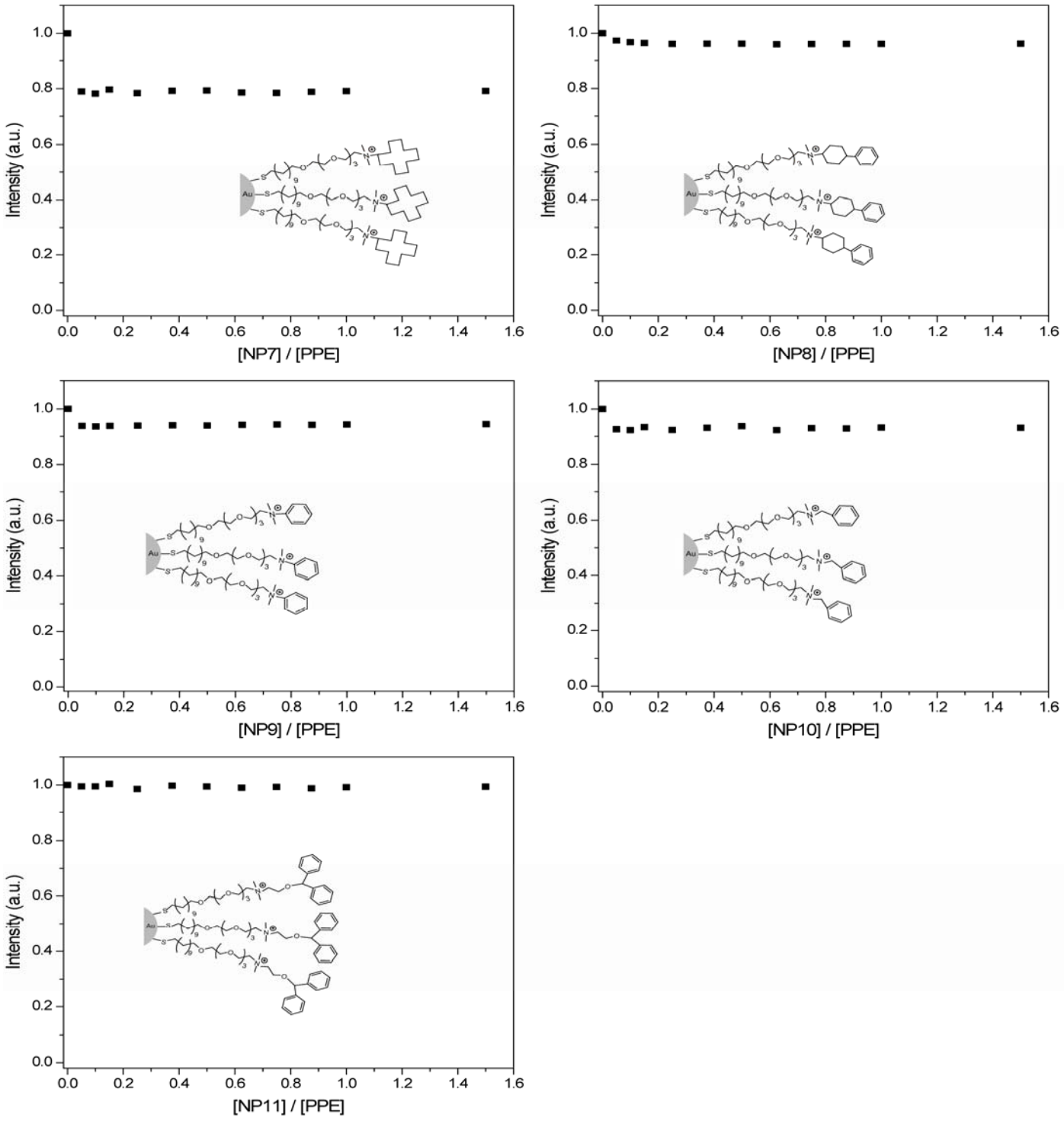

Figure S5. Fluorescence titration curves for the complexation of **NP_1-NP_{11}** with **S w-CO_2** in PB with 500 mM NaCl. The changes in fluorescence intensity at 465 nm were measured following the addition of cationic nanoparticles with an excitation wavelength of 405 nm.

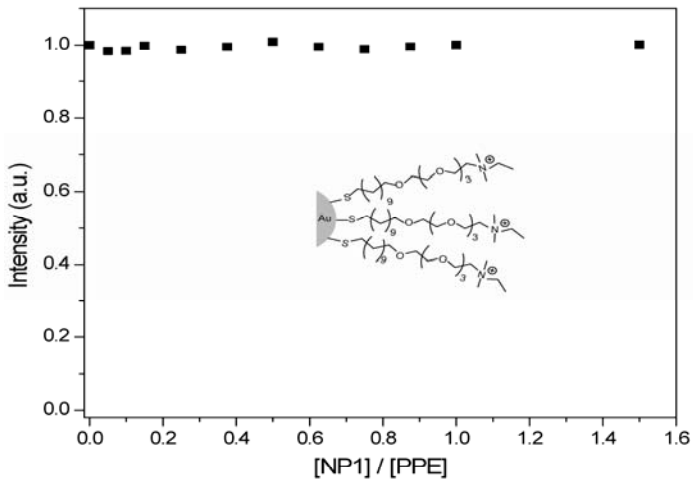
Intensity (a.u.)
[NP1] / [PPE]

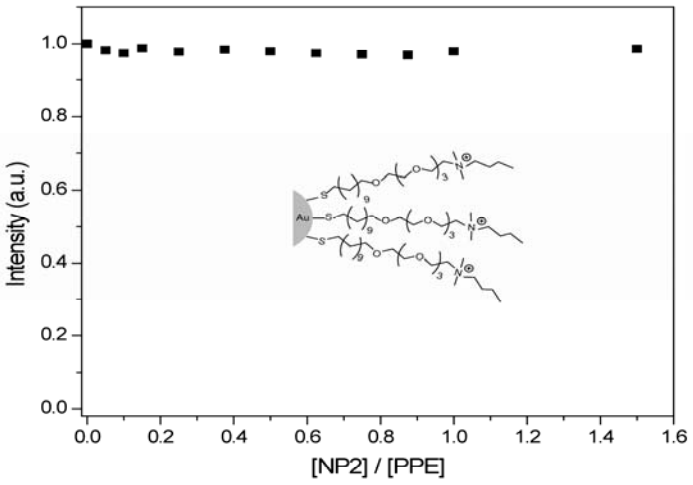
Intensity (a.u.)
[NP2] / [PPE]

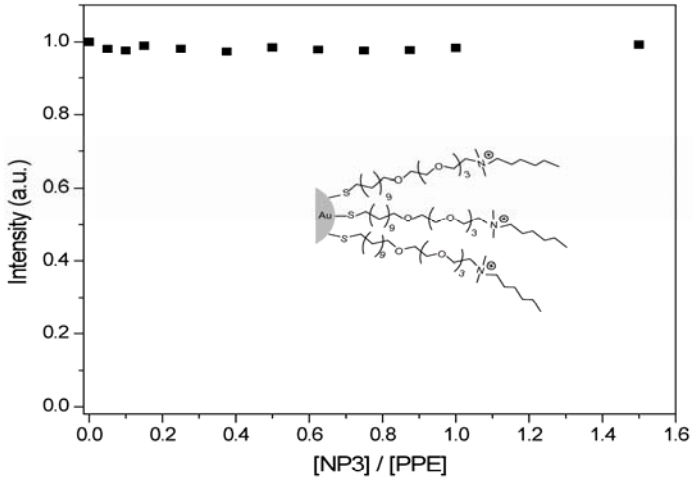
Intensity (a.u.)
[NP3] / [PPE]

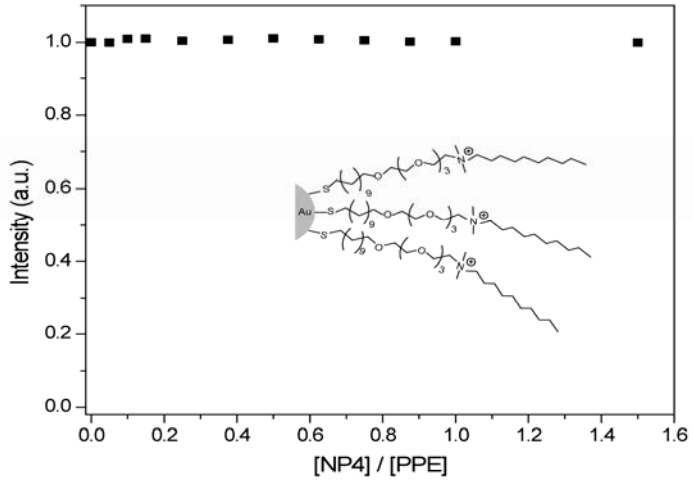
Intensity (a.u.)
[NP4] / [PPE]

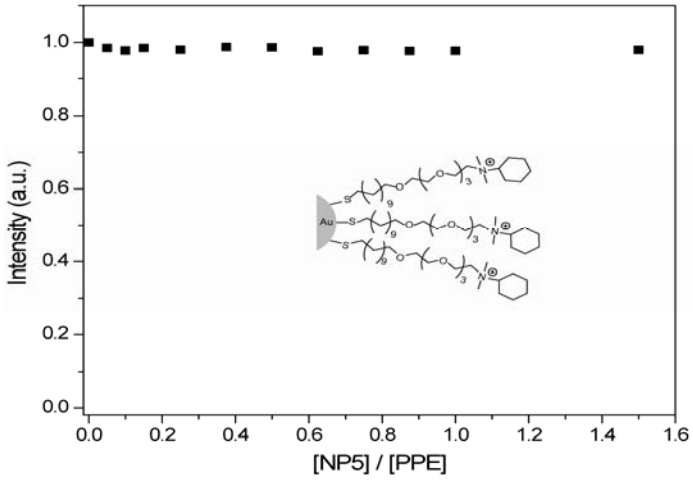
Intensity (a.u.)
[NP5] / [PPE]

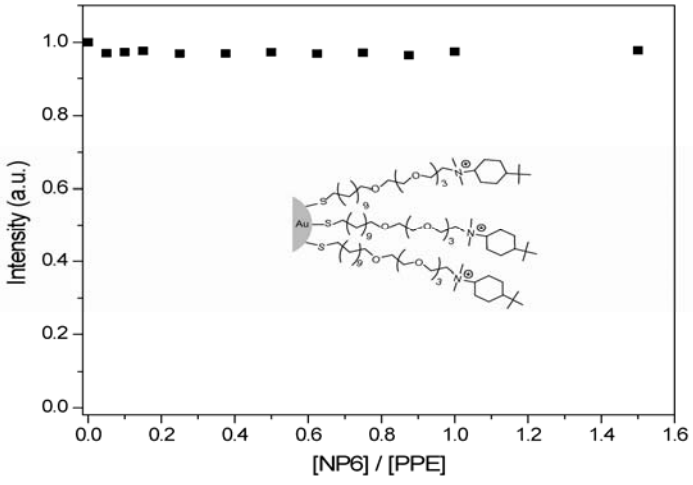
Intensity (a.u.)
[NP6] / [PPE]

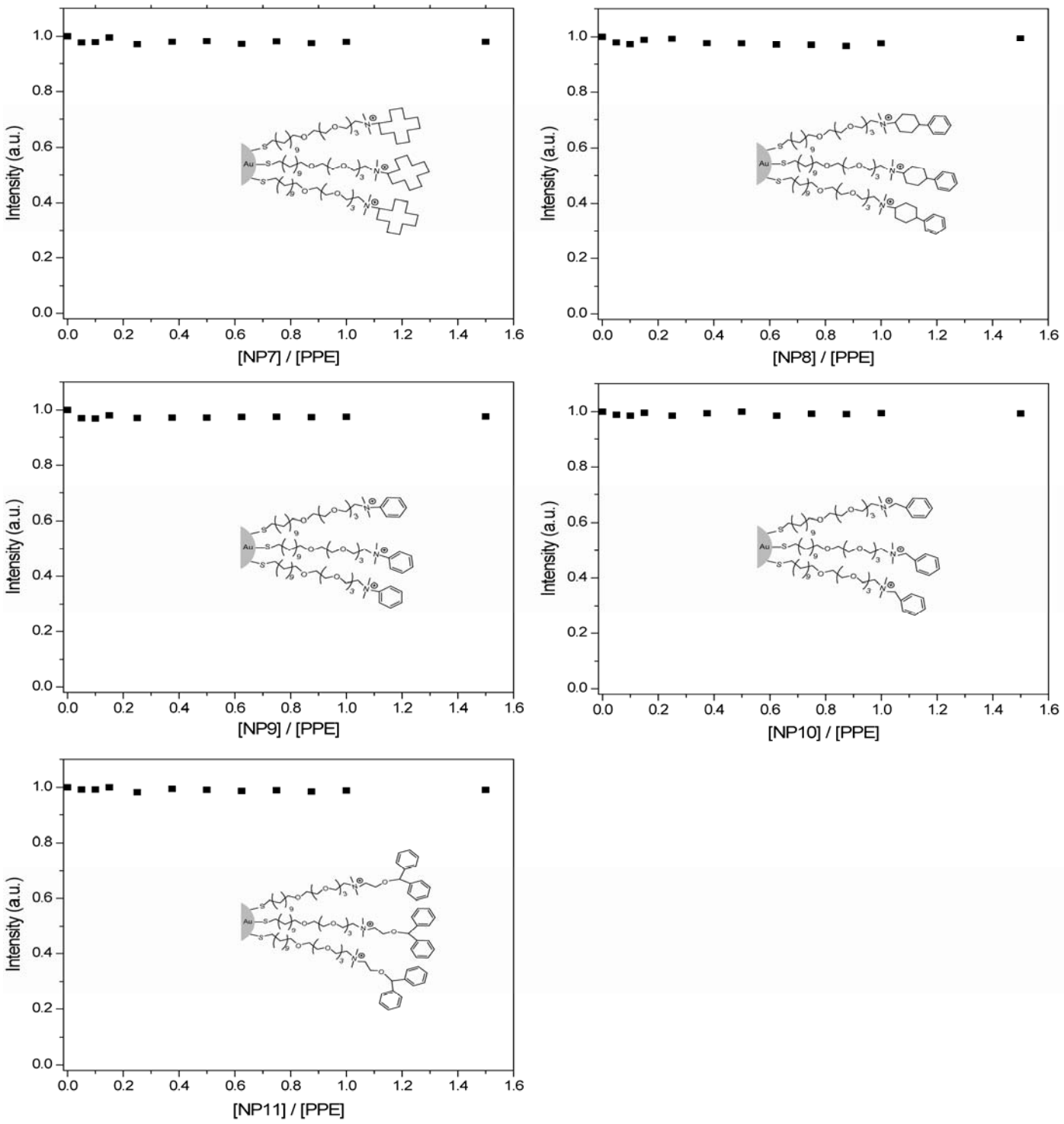

Figure S6. Fluorescence titration curves for the complexation of $\mathbf{NP_1}$-$\mathbf{NP_{11}}$ with $\mathbf{Sw\text{-}CO_2}$ in PB with 1000 mM NaCl. The changes in fluorescence intensity at 465 nm were measured following the addition of cationic nanoparticles with an excitation wavelength of 405 nm.

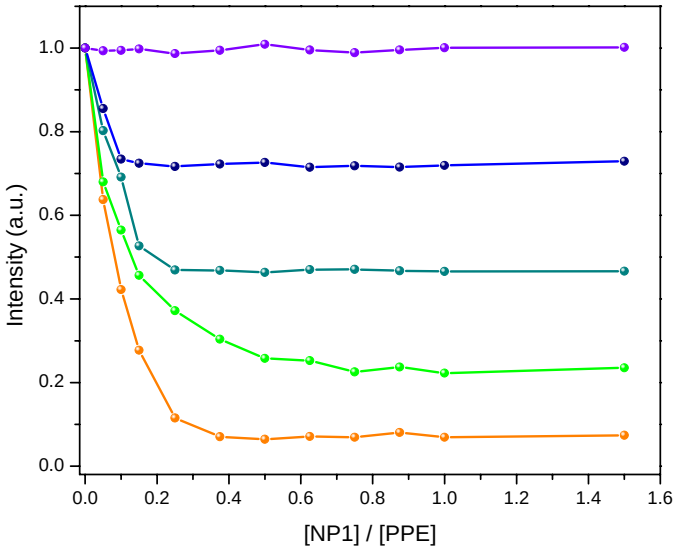
Intensity (a.u.)
[NP1] / [PPE]

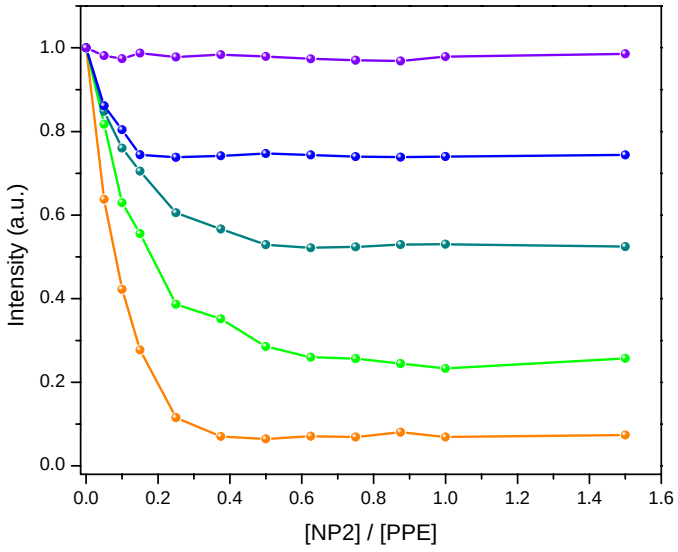
Intensity (a.u.)
[NP2] / [PPE]

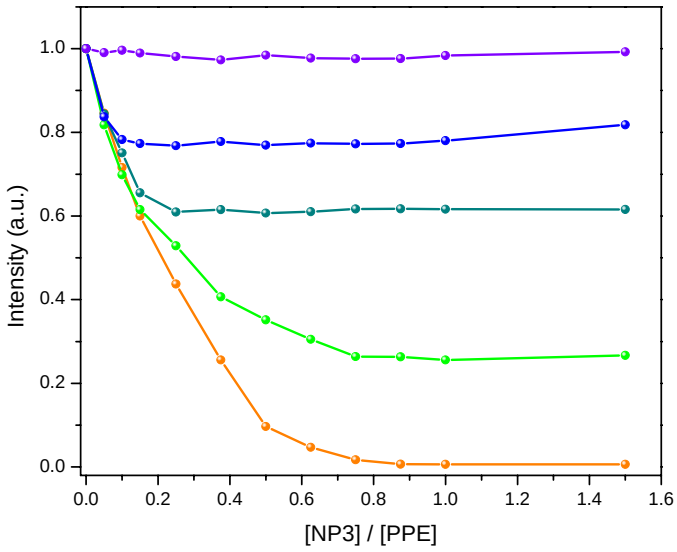
Intensity (a.u.)
[NP3] / [PPE]

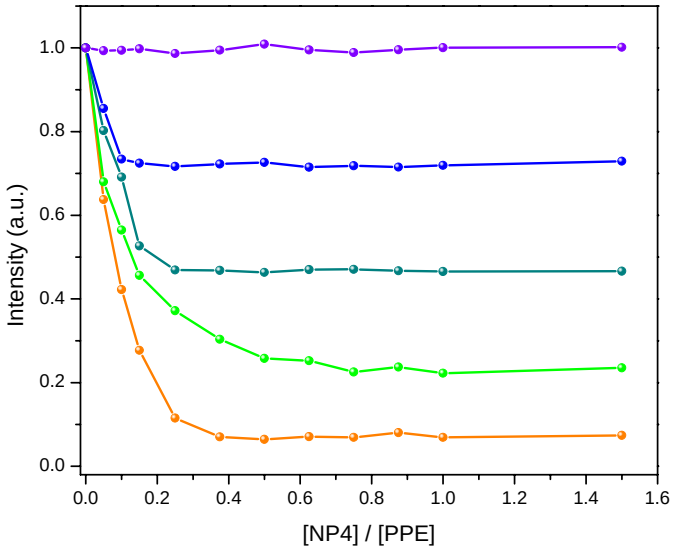
Intensity (a.u.)
[NP4] / [PPE]

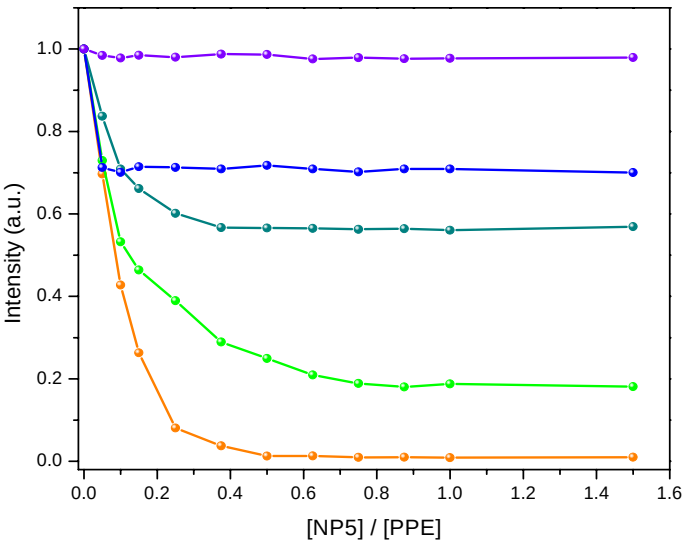
Intensity (a.u.)
[NP5] / [PPE]

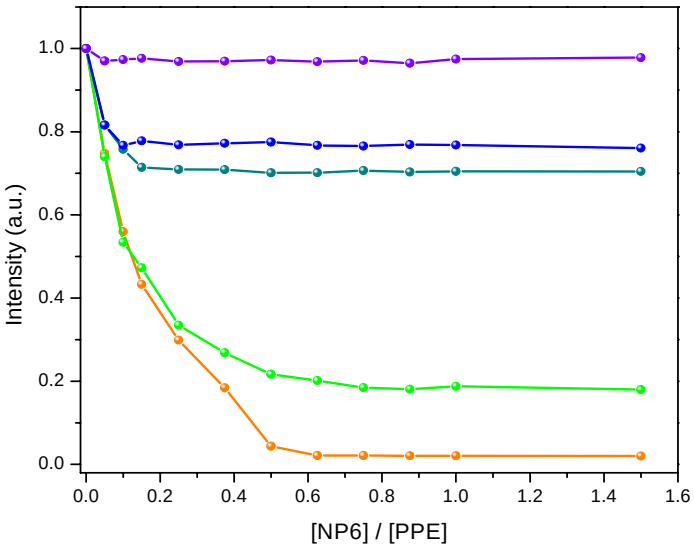
Intensity (a.u.)
[NP6] / [PPE]

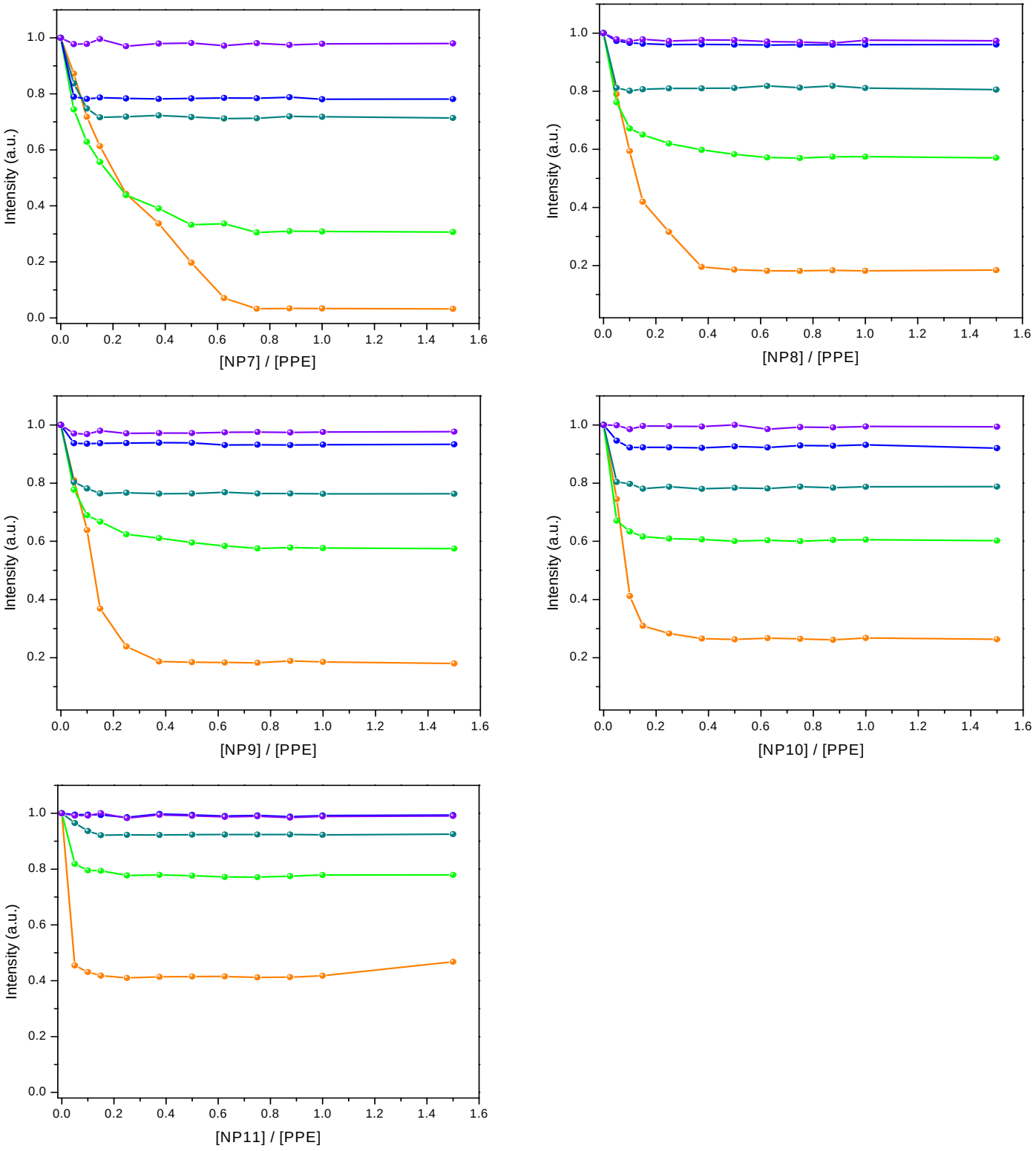

Figure S7. Overlap of fluorescence titration curves for the complexation of **NP_1-NP_{11}** with **Sw-CO_2** in PB with 0, 100, 250, 500, and 1000 mM NaCl. The changes in fluorescence intensity at 465 nm were measured following the addition of cationic nanoparticles with an excitation wavelength of 405 nm. Legend: Orange (0 mM NaCl), green (100 mM NaCl), dark cyan (250 mM NaCl), blue (500 mM NaCl) and violet (1000 mM NaCl)

Table S1. K_a and ΔG values for the complexation of **NP_1-NP_{11}** with **Sw-CO_2** in PB with 0, 100, 250, 500, and 1000 mM NaCl. At higher NaCl concentrations, values could not be accurately determined for all nanoparticle-conjugated polymer constructs.

Buffer	Nanoparticle	n	α	K_a (M^{-1})	ΔG (kJ / K*mol)
PB (0mM NaCl)	1	2.89	-1.07E+07	7.46E+07	-44.6
PB (0mM NaCl)	2	7.28	-1.02E+07	7.58E+07	-44.6
PB (0mM NaCl)	3	4.61	-1.01E+07	8.75E+07	-45.0
PB (0mM NaCl)	4	3.65	-1.09E+07	2.71E+07	-42.1
PB (0mM NaCl)	5	5.71	-9.97E+06	1.26E+08	-45.9
PB (0mM NaCl)	6	10.4	9.93E+06	1.85E+07	-41.1
PB (0mM NaCl)	7	12.9	-9.61E+06	4.21E+07	-43.2
PB (0mM NaCl)	8	5.96	9.43E+06	1.09E+08	-45.5
PB (0mM NaCl)	9	6.14	-9.28E+06	7.75E+08	-50.4
PB (0mM NaCl)	10	5.98	-9.26E+06	1.31E+09	-51.7
PB (0mM NaCl)	11	5.74	-9.24E+06	1.04E+10	-56.8
PB (100mM NaCl)	1	2.43	-9.11E+06	2.54E+06	-36.3
PB (100mM NaCl)	2	6.84	-9.12E+06	3.39E+06	-37.0
PB (100mM NaCl)	3	4.29	-9.11E+06	5.62E+06	-38.2
PB (100mM NaCl)	4	3.36	-9.08E+06	8.37E+06	-39.2
PB (100mM NaCl)	5	5.49	-9.01E+06	6.24E+07	-44.2
PB (100mM NaCl)	6	9.7	-8.98E+06	7.91E+06	-39.1
PB (100mM NaCl)	7	12.1	-8.73E+06	4.82E+06	-37.9
PB (100mM NaCl)	8	5.43	-8.61E+06	9.70E+06	-39.6
PB (100mM NaCl)	9	5.87	-8.49E+06	1.60E+07	-40.8
PB (100mM NaCl)	10	5.63	-8.47E+06	3.09E+08	-48.1
PB (100mM NaCl)	11	5.48	-8.43E+06	8.57E+08	-50.6
PB (250mM NaCl)	1	2.09	-7.97E+06	2.47E+05	-30.6
PB (250mM NaCl)	2	6.37	-7.95E+06	5.35E+05	-32.5
PB (250mM NaCl)	3	3.83	-7.99E+06	7.21E+05	-33.2
PB (250mM NaCl)	4	3.18	-7.92E+06	4.97E+05	-32.3
PB (250mM NaCl)	5	4.98	-7.89E+06	7.46E+06	-38.9
PB (250mM NaCl)	6	9.25	-7.85E+06	4.65E+05	-32.1
PB (250mM NaCl)	7	11.4	-7.69E+06	1.38E+05	-29.1
PB (250mM NaCl)	8	5.09	-7.54E+06	5.48E+05	-32.5
PB (250mM NaCl)	9	5.21	-7.47E+06	6.13E+06	-38.4
PB (250mM NaCl)	10	5.13	-7.42E+06	1.39E+06	-34.8
PB (250mM NaCl)	11	5.03	---	---	---

Buffer	Nanoparticle	n	α	K_a (M^{-1})	∆G (kJ / K*mol)
PB (500mM NaCl)	1	1.89	-7.29E+06	2.21E+03	-19.0
PB (500mM NaCl)	2	5.92	-7.28E+06	3.27E+03	-19.9
PB (500mM NaCl)	3	3.51	-7.24E+06	4.34E+03	-20.6
PB (500mM NaCl)	4	2.78	-7.22E+06	3.09E+03	-19.8
PB (500mM NaCl)	5	4.46	-7.19E+06	7.29E+03	-21.9
PB (500mM NaCl)	6	8.84	-7.17E+06	2.94E+03	-19.7
PB (500mM NaCl)	7	10.3	-6.99E+06	1.01E+03	-17.0
PB (500mM NaCl)	8	---	---	---	---
PB (500mM NaCl)	9	---	---	---	---
PB (500mM NaCl)	10	---	---	---	---
PB (500mM NaCl)	11	---	---	---	---
PB (1000mM NaCl)	1	---	---	---	---
PB (1000mM NaCl)	2	---	---	---	---
PB (1000mM NaCl)	3	---	---	---	---
PB (1000mM NaCl)	4	---	---	---	---
PB (1000mM NaCl)	5	---	---	---	---
PB (1000mM NaCl)	6	---	---	---	---
PB (1000mM NaCl)	7	---	---	---	---
PB (1000mM NaCl)	8	---	---	---	---
PB (1000mM NaCl)	9	---	---	---	---
PB (1000mM NaCl)	10	---	---	---	---
PB (1000mM NaCl)	11	---	---	---	---

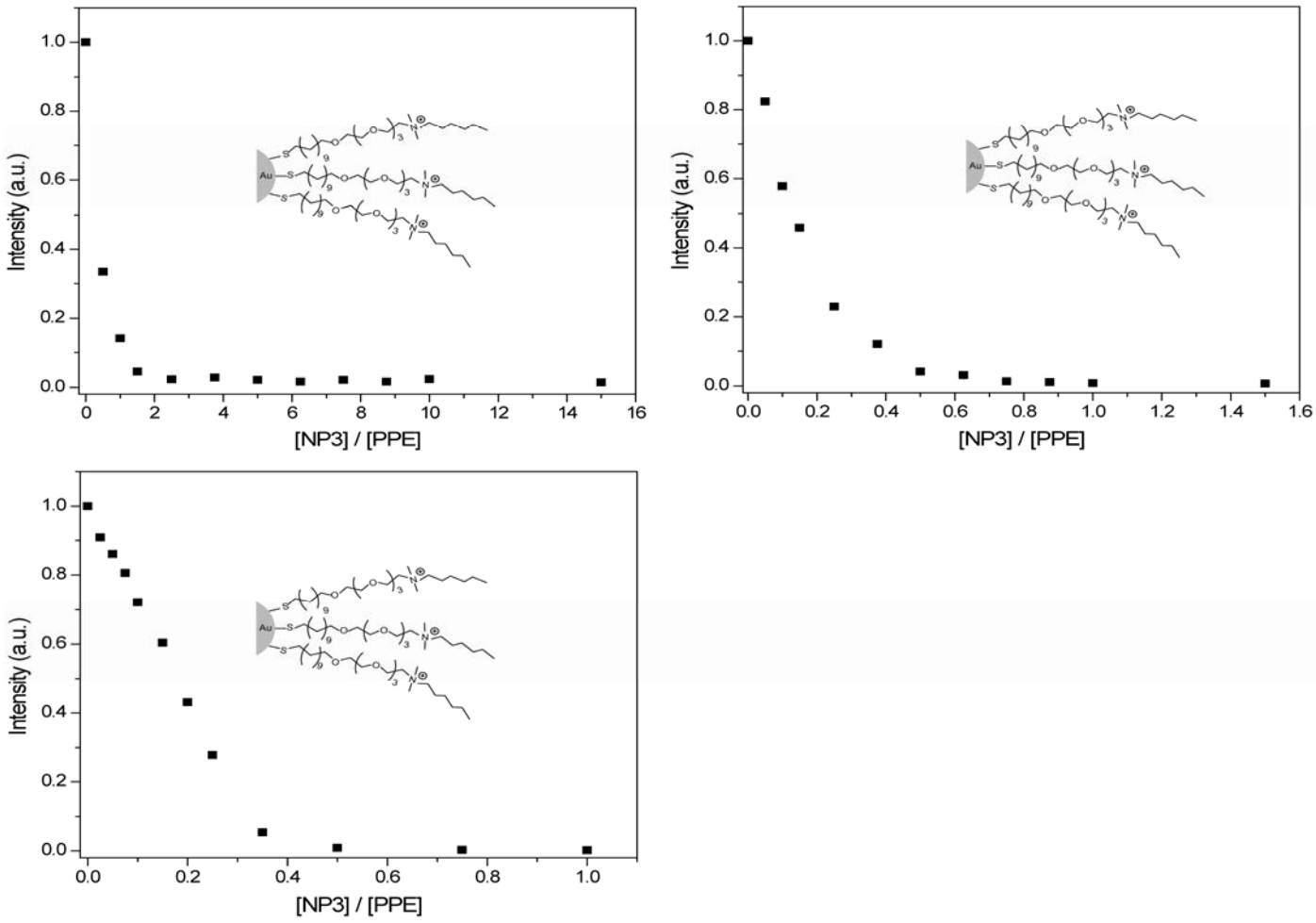

Figure S8. Fluorescence titration curves for the complexation of **NP_3** with 10 nM (top left), 100 nM (top right), and 1000 nM (bottom left) **Sw-CO_2.** The changes in fluorescence intensity at 465 nm were measured following the addition of cationic nanoparticles with an excitation wavelength of 405 nm.

Table S2. K_a and ΔG values for the complexation of **NP_3** with 10, 100, and 1000 nM **Sw-CO_2** in PB.

[PPE] (nM)	NP	K_a (M^{-1})	Delta G (kJ / K*mol)
10	3	8.63E+07	-45.0
100	3	8.75E+07	-45.0
1000	3	8.51E+07	-44.9

References:

1. Kim, I.B.; Phillips, R.L.; Bunz, U.H.F. *Macromolecules* **2007**, 40, 5290-5293.
2. You, C.-C.; Miranda, O.R.; Ghosh, P.S.; Kim, I.B.; Erdogan, B.; Krovi, S.A.; Bunz, U.H.F.; Rotello, V.M. *Nat. Nanotechnol*. **2007**, *2*, 318-323.
3. Brust, M.; Walker, M.; Bethell, D.; Schiffrin, D.J.; Whyman, R. *J. Chem. Soc., Chem. Commun*. **1994**, 801-802.
4. Hostetler, M.J.; Templeton, A.C.; Murray, R.W. *Langmuir* **1999**, 15, 3782-3789.